

See discussions, stats, and author profiles for this publication at: <https://www.researchgate.net/publication/8156975>

A Proficient Enzyme: Insights on the Mechanism of Orotidine Monophosphate Decarboxylase from Computer Simulations

ARTICLE in JOURNAL OF THE AMERICAN CHEMICAL SOCIETY · JANUARY 2005

Impact Factor: 12.11 · DOI: 10.1021/ja0455143 · Source: PubMed

CITATIONS

24

READS

17

3 AUTHORS:



Simone Raugei

Pacific Northwest National Laboratory

96 PUBLICATIONS 1,710 CITATIONS

SEE PROFILE



Michele Cascella

University of Oslo

53 PUBLICATIONS 856 CITATIONS

SEE PROFILE



Paolo Carloni

Forschungszentrum Jülich

320 PUBLICATIONS 6,036 CITATIONS

SEE PROFILE

A Proficient Enzyme: Insights on the Mechanism of Orotidine Monophosphate Decarboxylase from Computer Simulations

Simone Raugei,* Michele Cascella, and Paolo Carloni

Contribution from the International School for Advanced Studies (SISSA/ISAS) and INFN-DEMOCRITOS Modeling Center for Research in Atomistic Simulation, Via Beirut 2-4, 34014-Trieste, Italy

Received July 26, 2004; E-mail: raugei@sissa.it

Abstract: Decarboxylation of orotidine 5'-monophosphate (Omp) to uridine 5'-monophosphate by orotidine 5'-monophosphate decarboxylase (ODCase) is currently the object of vivid debate. Here, we clarify its enzymatic activity with long time scale classical molecular dynamics and hybrid ab initio Car–Parrinello/molecular mechanics simulations. The lack of structural (experimental) information on the ground state of ODCase/Omp complex is overcome by a careful construction of the model and the analysis of three different strains of the enzyme. We find that the ODCase/substrate complex is characterized by a very stable charged network Omp–Lys–Asp–Lys–Asp, which is incompatible with the previously proposed direct decarboxylation driven by a ground-state destabilization. A direct decarboxylation induced by a transition-state electrostatic stabilization is consistent with our findings. The calculated activation free energy for the direct decarboxylation with the formation of a C6 carboanionic intermediate yields an overall rate enhancement by the enzyme ($k_{\text{cat}}/k_{\text{wat}} = 3.5 \times 10^{16}$) in agreement with experiments ($k_{\text{cat}}/k_{\text{wat}} = 1.7 \times 10^{17}$). The decarboxylation is accompanied by the movement of a fully conserved lysine residue toward the developing negative charge at the C6 position.

I. Introduction

The enzyme orotidine 5'-monophosphate decarboxylase (ODCase) catalyzes the decarboxylation of orotidine 5'-monophosphate (Omp, Figure 1) to a major precursor in the formation of pyrimidine nucleotides, uridine 5'-monophosphate (Ump).^{1–6} In yeast and bacteria, ODCase is a single function protein, whereas in mammals the enzyme that catalyzes Omp decarboxylation is part of a bifunctional enzyme, which also catalyzes the preceding reaction (the transfer of ribose 5-phosphate to orotate to form Omp).⁷ ODCase is one of the most proficient enzymes, enhancing the rate of spontaneous substrate decarboxylation by more than 17 orders of magnitude. Its remarkable catalytic power is entirely dependent on noncovalent binding forces and does not involve metals or other cofactors.⁸ This is a very unusual characteristic among decarboxylating enzymes.³

The structure of ODCase from four different organisms has been determined by X-ray crystallography: *Methane bacterium thermoautotrophicum* (MBTO),⁹ yeast *Saccharomyces cerevi-*

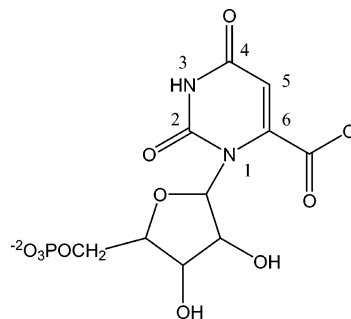


Figure 1. Structure of orotidine-5'-monophosphate.

siae (YEO),¹⁰ *Escherichia coli* (ECO),¹¹ and *Bacillus subtilis*.¹² These enzymes have a dimeric structure with an active site in each subunit, which acts independently.¹³ ODCase adopts an α/β -barrel fold with the ligand binding site consisting of residues belonging to both subunits of the active homodimer. The active site is characterized by a specific Lys–Asp–Lys–Asp array close to the carbon atom C6 of the substrate (Lys42–Asp70–Lys72–Asp75B in the MBTO numbering). Recent mutagenesis studies convincingly indicate that the residues of the conserved array are ionized and form an alternated charged network around

- (1) Orotidine Monophosphate Decarboxylase: A Mechanistic Dialogue. *Topics in Current Chemistry*; Lee, J. K., Tantillo, D. J., Eds.; Springer-Verlag: New York, 2004; Vol. 328. This volume contains six articles on recent advances in the study of ODCase.
- (2) Lee, J. K.; Tantillo, D. J. Computational Studies on the Studies on the Mechanism of Orotidine Monophosphate Decarboxylase. In *Advances in Physical Chemistry*; Richard, J. P., Ed.; Academic Press: New York, 2003; Vol. 38.
- (3) Miller, B. G.; Wolfenden, R. *Annu. Rev. Biochem.* **2002**, *71*, 847.
- (4) Ouchi, A. M. *Chem. Eng. News* **2000**, *78*, 42.
- (5) Chin, G. *Science* **2000**, *288*, 401.
- (6) Stubbe, J.; Johnson, L. N. *Curr. Opin. Struct. Biol.* **2000**, *10*, 709.
- (7) Yablonski, M. J.; Pasek, D. A.; Han, M. E. J. B.-D.; Traut, T. W. *J. Biol. Chem.* **1996**, *271*, 10704.
- (8) Radzicka, A.; Wolfenden, R. *Science* **1995**, *267*, 90.

- (9) Wu, N.; Mo, Y.; Gao, J.; Pai, E. F. *Proc. Natl. Acad. Sci. U.S.A.* **2000**, *97*, 2017.
- (10) Miller, B. G.; Hassell, A. M.; Wolfenden, R.; Milburn, M. V.; Short, S. A. *Proc. Natl. Acad. Sci. U.S.A.* **2000**, *97*, 2011.
- (11) Harris, P.; Poulsen, J.-C. N.; Jensen, K. F.; Larsen, S. *Biochemistry* **2000**, *39*, 4217.
- (12) Appleby, T. C.; Kinsland, C.; Begley, T. P.; Ealick, S. E. *Proc. Natl. Acad. Sci.* **2000**, *97*, 2005.
- (13) Porter, D. J. T.; Short, S. A. *Biochemistry* **2000**, *39*, 11788.

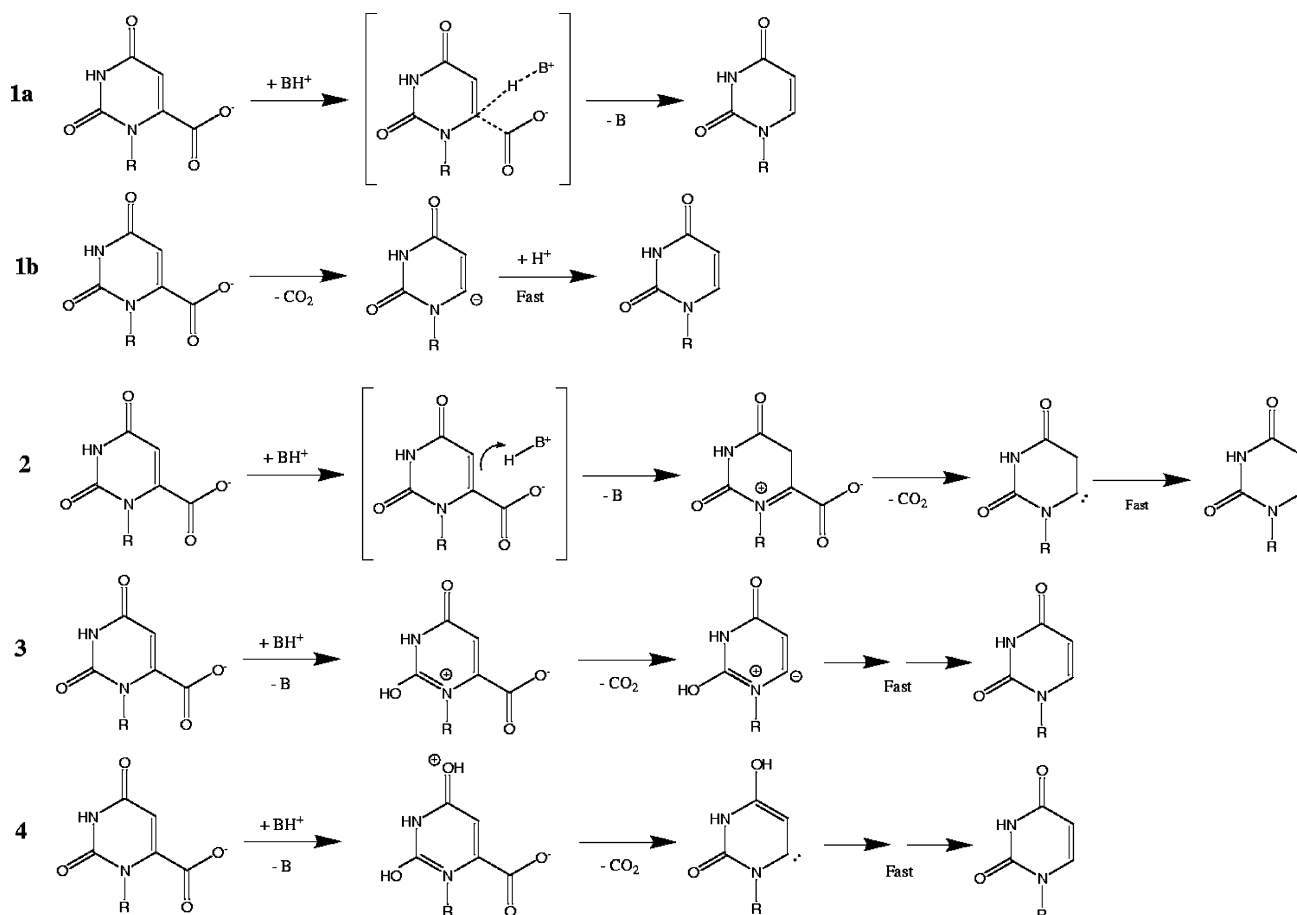


Figure 2. Proposed decarboxylation mechanisms. (1a) C6 protonation accompanied by decarboxylation; (1b) simple direct decarboxylation; (2) C5 protonation; (3) O2 protonation; (4) O4 protonation.

the reactive part of the substrate.¹⁴ In addition, one or more arginine residues form a salt bridge to the substrate's phosphate tail; other polar and ionizable groups are located in the binding pocket of both the phosphate group and the sugar ring.

Currently, the most accredited mechanisms involve a direct decarboxylation of Omp (Figure 2, reaction 1).³ This proposal is based on the analysis of the X-ray structure of ODCase-inhibitor complexes^{9,11,12,14–18} and is supported by a wealth of theoretical and experimental studies.^{9,19–21} Within this picture, the protonation/decarboxylation of Omp could be a concerted event (Figure 2, reaction 1a), as suggested by Harris et al.¹¹ and substantiated by the fact that incubation of the enzyme with Ump and CO₂ at pH = 8 does not result in any exchange of the C6 proton.¹⁷ This finding could imply that upon direct decarboxylation the formed (vinyl) carboanion intermediate is too unstable to be stabilized by the adjacent protonated lysine. In contrast, some other experimental evidence supports the formation of a carboanionic intermediate upon decarboxylation

(Figure 2, reaction 1b). For example, the observation of a favorable interaction between the $-O^-$ of the inhibitor 6-hydroxyuridine 5'-phosphate (BMP) in the ECO/BMP complex may imply a high affinity between the enzyme and the negative charge generated at C6.^{10,22} In both cases, kinetic studies have unambiguously identified Lys72 (MTBO numbering) as the residue that protonates the C6 center.^{3,14,23}

The remarkable proficiency of the enzyme has been suggested to be caused by either ground-state destabilization (GSD mechanism) (Figure 3) or transition-state stabilization (TSS). In the first hypothesis, as suggested by X-ray crystallography data,^{9,12} kinetic ¹⁵N and ¹³C isotope effects,²⁴ and free energy and binding energy calculations,⁹ the electrostatic repulsion between the substrate and the nearby Asp70 carboxylate would drive the decarboxylation.^{3,9,17} This repulsion would be counterbalanced by the favorable binding of the phosphate tail. However,^{19,20} this experimentally inferred energy gain is about 63 kJ mol⁻¹,^{10,22,25} that is, only 30 kJ mol⁻¹ larger than the overall substrate binding energy.³ This is not enough to compensate the electrostatic strain associated with a GSD mechanism, which should amount to 135 kJ mol⁻¹ to explain the observed rate acceleration.^{3,19,22} In addition, the GSD mechanism does not fully explain the profile of inhibitor binding

(14) Wu, N.; Gillon, W.; Pai, E. F. *Biochemistry* **2001**, *40*, 4002.

(15) Feng, W. Y.; Austin, T. J.; Chew, F.; Gronert, S.; Wu, W. *Biochemistry* **2000**, *39*, 1778.

(16) Houk, K. N.; Lee, J. K.; Tantillo, D. J.; Bahmanyar, S.; Hietbrink, B. N. *ChemBioChem* **2001**, *2*, 113.

(17) Begley, T. P.; Appleby, T. C.; Ealick, S. E. *Curr. Opin. Struct. Biol.* **2000**, *10*, 711.

(18) Wu, N.; Pai, E. F. *J. Biol. Chem.* **2002**, *277*, 28080.

(19) Warshel, A.; Strajbl, M.; Villà, J.; Florian, J. *Biochemistry* **2000**, *39*, 14728.

(20) Hur, S.; Bruce, T. C. *Proc. Natl. Acad. Sci. U.S.A.* **2002**, *99*, 9668.

(21) Lee, T.-S.; Chong, L. T.; Chodera, J. D.; Kollman, P. J. *Am. Chem. Soc.* **2001**, *123*, 12837.

(22) Miller, B. G.; Snider, M. J.; Short, S. A.; Wolfenden, R. *Biochemistry* **2000**, *39*, 8113.

(23) Smiley, J. A.; Jones, M. E. *Biochemistry* **1992**, *31*, 12162.

(24) Rishavy, M. A.; Cleland, W. W. *Biochemistry* **2000**, *39*, 4569.

(25) Miller, B. G.; Butterfoss, G. L.; Short, S. A.; Wolfenden, R. *Biochemistry* **2001**, *40*, 6227.

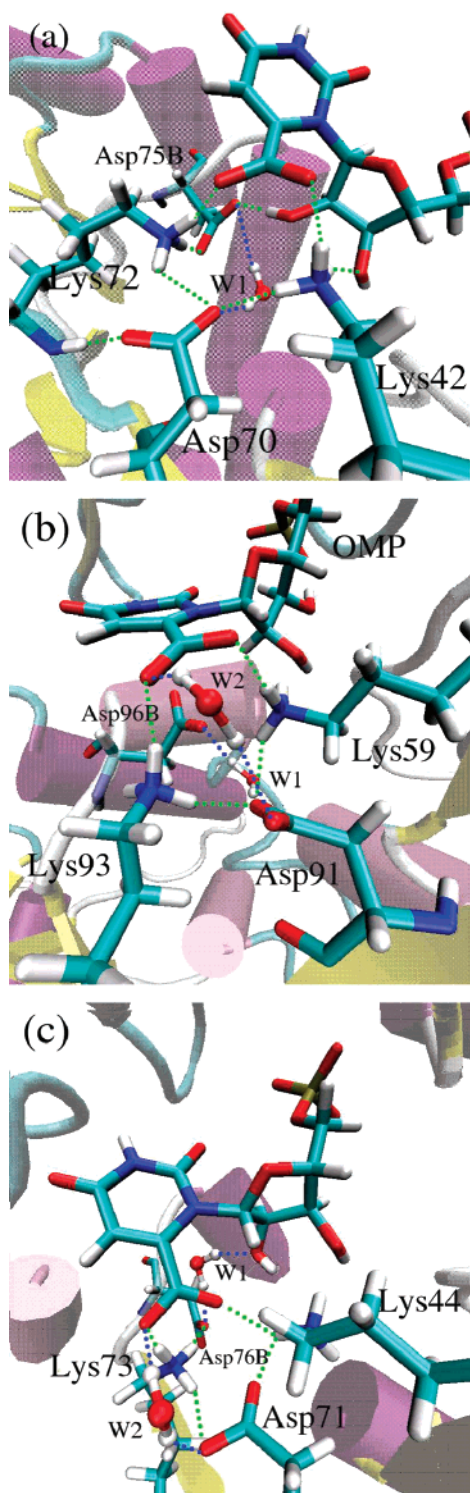


Figure 3. Snapshot of the ODCase/Omp complex ground state. (a) ODCase from *Methane bacterium thermoautotrophicum* (MTBO); (b) ODCase from yeast *Saccharomyces cerevisiae* (YEO); (c) ODCase from *Escherichia Coli* (ECO).

affinities where the negative charge at the C6 position is preferred to the neutral one.²⁶

The second proposal, based on EVB free energy perturbation simulations and binding energies affinities carried out by Warshel and co-workers,¹⁹ suggests that the electrostatic field

of the charged residues adjacent to the Omp carboxylate is already organized in a such a way to be complementary to the transition-state (TS) charge distribution. In particular, from the calculation of binding affinities, these authors concluded that the binding affinity of the TS is higher than that of the ground state.

More recently, Hur and Bruice,²⁰ studying YEO by molecular dynamics, have advanced the idea that the decarboxylation results from both stabilization of the carboanionic intermediate by a nearby lysine of the conserved array upon decarboxylation and reorganization of the 203–218 loop. Because the intermediate and the TS have similar energy, the stabilization of the former reduces the free energy of the latter.

Another recently proposed catalytic mechanism assumes a preliminary protonation of the uracil ring far from the decarboxylation center. Kollman,²¹ assuming a protonated Asp70, proposed as a first step of the decarboxylation an interesting mechanism involving an enamine protonation at C5 carried out by the residue Lys72 (according to the MBTO numbering, Figure 2, reaction 2). As yet, no experimental studies have been dedicated to the assessment of this mechanism.

Herein, we reexamine these hypotheses by extensive classical molecular dynamics simulations and current state of the art of ab initio (Car–Parrinello) molecular mechanics (QM/MM) simulations.^{27,28} Notice that we do not discuss here the proposal, based on ab initio calculations, that O2 and O4 are protonated prior to decarboxylation (Figure 2, reactions 3 and 4),^{29–32} as this hypothesis is not supported by the lack of sufficiently acidic groups¹¹ and mutagenesis experiments,²⁶ which exclude the possibility of proton-transfer relay from bulk water solvent.

Our calculations strongly support a direct decarboxylation of Omp with the formation of a carboanionic intermediate via a TSS mechanism, in which the fully conserved Lys72 (MTBO numbering) plays a fundamental role by stabilizing the forming negative charge at C6 and, consequently, the TS. In contrast, mechanisms involving a protonation at C5 or C6 of the substrate are very unlikely.

II. Computational Details

The study of the catalytic proficiency of ODCase was carried out in two distinct stages. In the first stage, classical molecular dynamics (section II.A) was used to sample the conformational space of enzyme/substrate complex. Next, hybrid QM/MM simulations (section II.B) were performed to reconstruct the free-energy profile along the relevant reaction coordinate of the most accredited decarboxylation routes. Because bond breaking and forming require the crossing of a relatively large activation barrier, a method to sample the relevant reaction coordinate must be employed.^{33–38} In the present study, we have used

(26) Miller, B. G.; Snider, M. J.; Wolfenden, R.; Short, S. A. *J. Biol. Chem.* **2001**, *276*, 15174.

(27) Laio, A.; VandeVondele, J.; Rothlisberger, U. *J. Chem. Phys.* **2002**, *116*, 6941.
 (28) Laio, A.; VandeVondele, J.; Rothlisberger, U. *J. Phys. Chem. B* **2002**, *106*, 7300.
 (29) Lee, J. K.; Houk, K. N. *Science* **1997**, *276*, 942.
 (30) Singleton, D. A.; Merrigan, S. R.; Kim, B. J.; Phillips, L. M.; Phillips, P. B.; Lee, J. K. *J. Am. Chem. Soc.* **2000**, *122*, 3296.
 (31) Phillips, L. M.; Lee, J. K. *J. Am. Chem. Soc.* **2001**, *123*, 12067.
 (32) Kurinovich, M. A.; Lee, J. K. *J. Am. Soc. Mass Spectrom.* **2002**, *13*, 985.
 (33) Jarzynski, C. *Phys. Rev. Lett.* **1997**, *78*, 2690.
 (34) Laio, A.; Parrinello, M. *Proc. Natl. Acad. Sci. U.S.A.* **2002**, *99*, 12562.
 (35) Passerone, D.; Parrinello, M. *Phys. Rev. Lett.* **2001**, *87*, 108302.
 (36) Elber, R. In *Recent Developments in Theoretical Studies of Proteins*; Elber, R., Ed.; World Scientific: River Edge, NJ, 1996; Chapter Reaction path studies of biological molecules.
 (37) Dellago, C.; Bolhuis, P. G.; Chandler, D. *J. Chem. Phys.* **1999**, *110*, 6617.
 (38) Sprik, M.; Ciccotti, G. *J. Chem. Phys.* **1998**, *109*, 7737.

Table 1. Root Mean Square Displacements (in Å) from an Equilibrium Structure of the Protein Skeleton (C_α), the Conserved Amino Acid Array, and the Two Omp Units along 8, 6, and 5 ns Trajectories for MTBO/Omp, YEO/Omp, and ECO/Omp, Respectively^a

	MTBO	YEO	ECO
ODcase	1.23 (0.13)	1.63 (0.21)	1.43 (0.16)
Asp—Lys—Asp—Lys	0.41 (0.06)	0.46 (0.05)	0.65 (0.09)
Omp	0.26 (0.06)	0.33 (0.06)	0.38 (0.09)

^a The standard deviation from the average is reported in parentheses.

the multiple steering molecular dynamics in a Car–Parrinello QM/MM framework,^{39,40} as briefly described in section II.C.

Because the two active sites are independent, we will explicitly take into account only subunit A.

A. Classical Molecular Dynamics. One of the difficulties encountered in studying the catalytic mechanism of ODCase is represented by the lack of information about the ground-state geometry of the enzyme/substrate complex. None of the X-ray structures available so far were crystallized with a carboxylated substrate. Hence, the spatial arrangement around the carboxylate group of Omp is not well determined. The situation is made more complicated by the structural diversity among the ODCase structures.^{9–12,14,18} To carry out an exhaustive and reliable study, we investigated three different strains: MBTO (Protein Data Bank, PDB, entry 1DVJ),⁹ YEO (PDB entry 1DQX),²² and ECO (PDB entry 1EIX).¹¹ Both of the adducts with Omp and Ump (C6) carboanion (Ump[−]), which is involved in the direct decarboxylation of the substrate without prior protonation, were taken into account.

The Omp structure was obtained from the inhibitors (6-aza-Ump, 6NU, and BMP) by replacing the N6 of 6NU in 1DVJ and C6-hydroxide oxygen of BMP in 1DQX and in 1EIX with a C6-carboxylate group.²¹ Following Hur and Bruice,²⁰ the enzyme/Ump complex was obtained by simply removing the carboxylate moiety from Omp. A geometry relaxation of the substrate molecules in the enzyme cavity was performed after building them.

All histidines were protonated at the N_δ as in refs 19 and 21. The conserved Lys–Asp–Lys–Asp, along with all of the other ionizable residues, was supposed to be fully ionized⁴¹ according to the latest experimental evidence.¹⁴ The Amber^{42,43} force field was used for the protein, water, and counterions. For Omp, we used the potential parameters developed by Lee et al.²¹ For Ump[−], we used stretching, bending, and torsional parameters developed for Omp, whereas its atomic point charges were calculated using the RESP scheme as in ref 21.

The ODCase/substrate complexes were enclosed in an orthorhombic cell and solvated by about 20 000 water molecules and Na⁺ counterions to ensure neutrality. The electrostatic was treated using particle mesh Ewald summation. The equilibration of the ODCase/Omp complexes was achieved by a 600 ps restrained molecular dynamics in which a harmonic potential of 20 kcal mol^{−1} Å^{−2} was applied to each atom and then gradually switched off. This allowed the protein structure to adjust very softly in the presence of the ligand. At the same time, the temperature was raised from 0 to 300 K using a stochastic rescaling of the atomic velocities and allowing to the cell to readjust its volume. Eventually, to avoid that the structure relaxed into a local minimum, several cycles of heating and cooling between 300 and 340 K have been performed. During these and in all of the further stages, temperature was controlled with the Berendsen thermostat of frequency 1 ps^{−1}. The system was then equilibrated for a further 300 ps, and the conformational space was then sampled for 5–8 ns, depending on the system.

The thermalization time was sufficiently long to have well-equilibrated structures, as can be inferred both from the root-mean-square displacement from the equilibrium structure (RMSD), which shows no appreciable drifts in the multiple nanosecond time scale (Table 1).

B. Hybrid Car–Parrinello/Molecular Mechanics Simulations.

Because these kinds of calculations are extremely expensive, we only focused on MBTO, which has been widely studied with ab initio methods.^{9,19,21}

To have an accurate description of the chemical processes involved, the QM region was composed by the entire Omp molecule and the Lys42–Asp70–Lys72–Asp75B network. The aspartyl and lysine residues were modeled as acetic anions and protonated methylamine, respectively. The covalent links between the QM and the MM regions were treated with the conventional capping procedure.⁴⁴ The electrostatic coupling between the QM and the MM region is calculated by using the fully Hamiltonian scheme proposed by Rothlisberger and co-workers^{27,28} as implemented in the Car–Parrinello code CPMD3.5.^{45,46} The reference reaction in water was studied by immersing Omp in a box of 628 water molecules and two counterions. The Omp molecule was treated at the QM level, while the rest were treated with the Amber force field.

In all of the systems, the quantum region was described within gradient-corrected DFT using the Becke⁴⁷ and Lee, Yang, and Parr⁴⁸ (BLYP) exchange and correlation energy functionals. Norm-conserving Martins–Troullier pseudo-potentials⁴⁹ were used to describe the interactions between the core and valence electrons for all atoms but for hydrogens, for which a Von Bart–Car-type pseudopotential was used to smooth out the short-range Coulombic nuclear potential. The Kohn–Sham orbitals of valence electrons were expanded in plane waves with a kinetic energy up to 70 Ry. A fictitious electronic mass of 400 au was used, which allowed an integration of the equations of motion with a time-step of 0.097 fs.

C. Free-Energy Calculations. The free-energy profile along selected reactive routes was calculated via nonequilibrium QM/MM molecular dynamics simulations. In the following paragraph, we will only recall the relevant concepts strictly necessary for the ensuing discussion. For a detailed description of this methodology, see refs 50–52.

- (40) Cascella, M.; Raugei, S.; Carloni, P. *J. Phys. Chem. B* **2004**, *108*, 369.
- (41) We remark that, in the present case, estimation of protonation states based on pK_a calculations is very sensitive to the protocol employed.^{19,21} As pointed out by one of the referees, Lee et al.²¹ found Asp70 to be neutral by MM/PBSA calculations, which have not been verified by proper pK_a in model systems. Thus, the use of such a technique may not be appropriate for pK_a evaluations in very polar environments such as the ODCase active site.
- (42) Case, D.; Pearlman, D.; Caldwell, J.; Cheatham, T., III; Wang, J.; Ross, W.; Simmerling, C.; Darden, T.; Merz, K.; Stanton, R.; Cheng, A.; Vincent, J.; Crowley, M.; Tsui, V.; Gohlke, H.; Radmer, R.; Duan, Y.; Pitera, J.; Massova, I.; Seibel, G.; Singh, U.; Weiner, P.; Kollman, P. *AMBER7*; University of California: San Francisco, CA, 2002.
- (43) Pearlman, D.; Case, D.; Caldwell, J.; Ross, W.; Cheatham, T., III; DeBolt, S.; Ferguson, D.; Seibel, G.; Kollman, P. *Comput. Phys. Commun.* **1995**, *91*, 1.
- (44) Sherwood, P. *NIC Series*; John von Neumann Institute for Computing: Jülich, 2000; Vol. 1, p 385.
- (45) Hutter, J.; Alavi, A.; Deutch, T.; Bernasconi, M.; Goedecker, S.; Marx, D.; Tuckerman, M.; Parrinello, M. *CPMD*; MPI für Festkörperforschung und IBM Zurich Research Laboratory, 1995–2002.
- (46) The electrostatic coupling between the QM and the MM regions is calculated by splitting the MM subsystem in three spherical regions centered on the QM part. The inner region consists of enzyme residues within 6 Å of the QM part, and the electrostatic interaction between this region and the QM area is directly computed as the interaction energy between the MM point charges and uniform QM charge density.²⁷ To avoid an unphysical charge escape from the QM region (the so-called spill-out problem), a short-range modified Coulomb interaction was used.²⁷ The middle region consists of all of the residues in the region between 6 and 18 Å, and the electrostatic interaction between the QM and this MM region is calculated as point charge–point charge interaction, where the charges associated to the QM part are calculated on-the-fly using the RESP scheme proposed by Laio et al.²⁸ Finally, the electrostatic interaction between the third region, which is composed by all of the remaining MM atoms, and the QM region is computed by a multipolar expansion of the QM charge density up to the quadrupole moment.²⁷
- (47) Becke, A. D. *Phys. Rev. A* **1988**, *38*, 3098.
- (48) Lee, C.; Yang, W.; Parr, R. G. *Phys. Rev. B* **1988**, *37*, 785.
- (49) Troullier, N.; Martins, J. L. *Phys. Rev. B* **1991**, *43*, 1993.
- (50) Hummer, G.; Szabo, A. *Proc. Natl. Acad. Sci. U.S.A.* **2001**, *98*, 3658.
- (51) Park, S.; Schulten, K. *J. Chem. Phys.* **2004**, *120*, 5946.
- (52) Israelowitz, B.; Gao, M.; Schulten, K. *Curr. Opin. Struct. Biol.* **2001**, *11*, 224.

(39) Cascella, M.; Guidoni, L.; Rothlisberger, U.; Maritan, A.; Carloni, P. *J. Phys. Chem. B* **2002**, *106*, 13027.

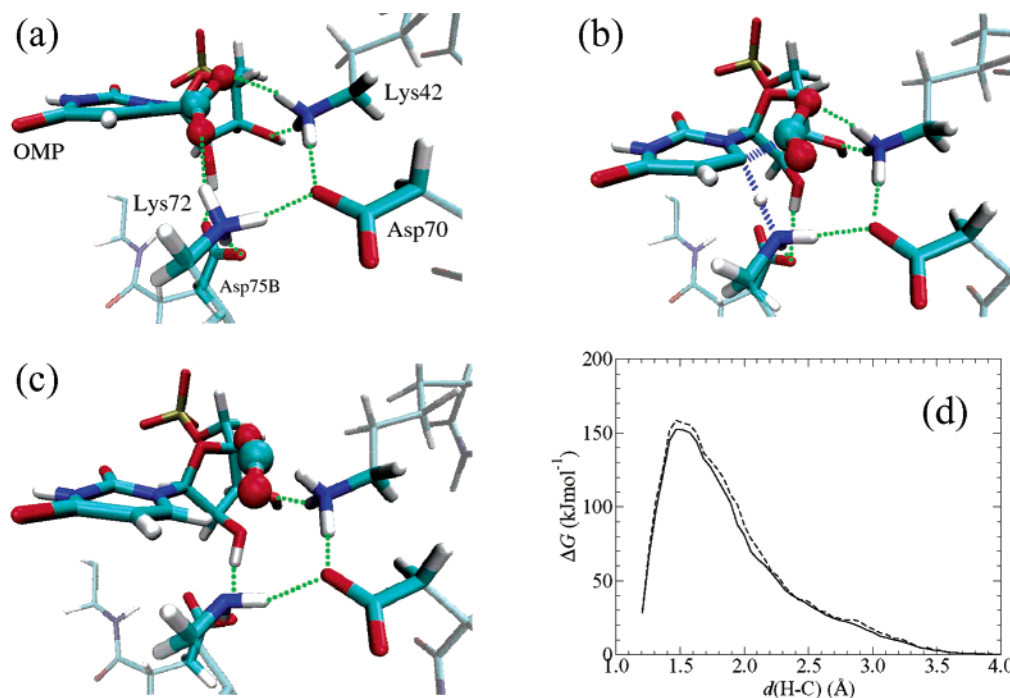


Figure 4. C6-protonation/decarboxylation reaction. (a) Reactants; (b) transition state; (c) products; (d) free energy profile (dashed line free energy obtained averaging over only one trajectory, see text). The part of the system treated ab initio is highlighted.

Let $H(\mathbf{r}, t)$ be the Hamiltonian of a system that is subject to an external time-dependent perturbation, and let $\Delta G(t)$ and $W(t)$ be, respectively, the change in free energy and the external work performed on the system as the system evolves from time zero to time t . Here, \mathbf{r} denotes a configuration of the whole system. According to Jarzynski,³³ $\Delta G(t)$ and $W(t)$ are related to each other by the following identity:

$$e^{-\beta\Delta G(t)} = \langle e^{-\beta W(t)} \rangle$$

where the brackets represent an average taken over an ensemble of trajectories.

In the present study, we induced a chemical transformation, adding to the Hamiltonian of the system, $H_0(\mathbf{r})$, a time-dependent harmonic potential, whose minimum position moves at constant velocity v :⁵⁰

$$H(\mathbf{r}, t) = H_0(\mathbf{r}) + \frac{k}{2}[z(\mathbf{r}) - z_0 - vt]^2$$

where $z(\mathbf{r})$ represents a chosen reaction path. In this way, at any given time, only a small window around the equilibrium position $z(\mathbf{r}) = z_0 + vt$ was sampled. By using the Jarzynski equality,³³ from the average of the irreversible work over a number of representative (finite-time) transformations, it is possible to work out the free-energy change along the chosen reaction path:⁵³

$$G(z) = -\beta^{-1} \ln \langle \delta[z(\mathbf{r}(t)) - z] e^{-\beta W(t)} \rangle \quad (1)$$

To study the protonation at C6 with concomitant decarboxylation, the distance between C6 and a randomly chosen H atom bonded to Lys N ϵ nitrogen was used as the reaction coordinate, whereas to study the direct decarboxylation without prior protonation, we chose as the reaction coordinate the C–C bond distance. In both cases, the steering velocity and the harmonic constant were $v = 0.7 \text{ \AA ps}^{-1}$ and $k = 100$

$\text{kJ mol}^{-1} \text{ \AA}^{-2}$, respectively. For reference, the direct decarboxylation in aqueous solution was studied by using $k = 200 \text{ kJ mol}^{-1} \text{ \AA}^{-2}$.⁵⁴

For all of the reactions, the free-energy profile was computed by averaging the irreversible work over five trajectories. The initial configuration of each steering simulation was taken from a free 7 ps QM/MM simulation. The origins of these simulations were equispaced in time by about 0.8 ps. With this choice of both external perturbation and starting configurations, the reaction free energy converged within a few trajectories, as can be appreciated from Figures 4d and 5e.

III. Results and Discussion

A. Classical Molecular Dynamics. Structure of the Active Site. We find that the active site is characterized by remarkably strong $\text{Omp-COO}^- \cdots \text{N}_\epsilon\text{-Lys}$ interactions. Each of the two lysine residues of the conserved array is hydrogen bonded to one O-atom of the carboxylate moiety, as depicted in Figure 3. The strength of these salt-bridge-like H-bonds can be appreciated from the statistical data on distances between Omp-COO^- oxygens and $\text{N}_\epsilon\text{-Lys}$ atoms reported in Table 2. Furthermore, in all of the complexes, a water molecule links the Omp-COO^- to the other aspartyl residue of the conserved charged array belonging to the other subunit (molecule W1 in Figure 3). In ECO and YEO, a second water molecule was found in a bridging position between the substrate carboxyl group and the facing aspartyl group (molecule W2 in Figure 3). We found that these solvent molecules are relatively mobile as they are exchanged with surrounding molecules in the nanosecond time scale. These findings contrast with previous simulations where only Lys72 (MBTO numbering)^{9,19,21} or Lys93 (ECO numbering)²⁰ were reported to be H-bonded to the Omp carboxylate

(53) Equation 1 requires the convergence of an exponential. Therefore, to evaluate it, it is more convenient to use a second-order cumulant expansion:⁵⁰ $G(z') \approx -\beta^{-1} \ln \langle \delta[z(\mathbf{r}(t')) - z'] \rangle + \langle W(t') \rangle_{z'} - (\beta/2) \sigma^2 \langle W(t') \rangle_{z'}$, where $\langle \cdots \rangle_{z'}$ denotes an average restricted to trajectories satisfying the condition $z[\mathbf{r}(t')] = z'$ and σ^2 is the variance of the average work done.

(54) Notice that the convergence of the free energy profile does not depend on the harmonic force constant, k , if the latter is of the same magnitude of the energy barrier to be crossed and all of the degrees of freedom orthogonal to the chosen reaction coordinate relax faster than the dragging velocity v .^{39,40} We remark that the activation barriers in the enzyme cavity and in water solution (spontaneous decarboxylation) are about 72 and 164 kJ mol^{-1} , respectively.³

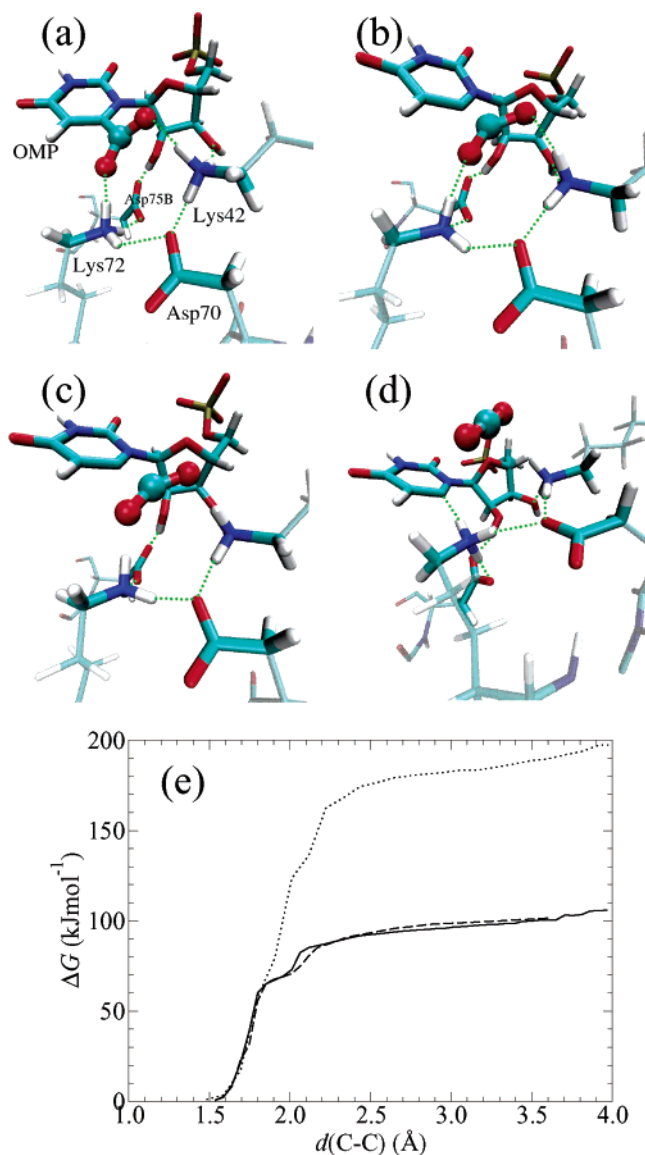


Figure 5. Direct decarboxylation. (a) Reactants; (b) breaking of the C–C bond; (c) breaking of the $\text{CO}_2 \cdots \text{H}(\text{Lys})_2$ H-bond; (d) intermediate; (e) free energy profiles. In (e), solid and dotted lines refer to the direct decarboxylation in the enzyme cavity and in aqueous solution, respectively (the dashed line is the free energy profile calculated averaging over only one trajectory, see text).

Table 2. Statistical Data on Distances (in Å) between the N_ϵ -Lys and the O Atom of the Omp-COO^- Moiety^a

		minimum	maximum	average
MTBO	Lys72	2.51	2.90	2.70 (0.08)
	Lys42	2.54	3.04	2.74 (0.09)
ECO	Lys59	2.47	2.95	2.76 (0.10)
	Lys93	2.53	3.13	2.79 (0.09)
YEO	Lys44	2.53	3.08	2.72 (0.08)
	Lys73	2.56	3.44	2.78 (0.10)

^a Standard deviation from the average (last column) is reported in parentheses.

group. In particular, in a previous 2 ns (CHARMM) simulation of YEO,²⁰ it was found that Omp-COO^- is bridged to the facing Asp91 by Lys93 and a water molecule.

The different active site structure between the present and previous simulations may be attributed to the different potential function or, more likely, to the different equilibration protocol

adopted and the much longer sampling time here covered. In particular, for what concerns the equilibration, the annealing cycles allowed the conserved charged array to softly readjust and find the optimal conformation. To further validate our findings, we carried out 1 ns simulations at 40, 60, and 80 °C. Only at a very high temperature does the hydrogen-bonding pattern change in the nanosecond time scale, and a conformation where either a lysine is bound to the same O-atom of the carbonyl Omp group, or a lysine (Lys42 in the MBTO numbering) flips and binds to an oxydriol group of the ribosil moiety, is achieved.

The stability of the charged array may be attributed to the alternated charge signs in the conserved network. In fact, the two positive lysines reduce the electrostatic repulsion between the Omp carboxyl group and the facing aspartyl residue. Furthermore, the two lysines and the bridging water molecule W1 mitigate the electrostatic repulsion between Omp and the aspartyl group belonging to the other subunit. All of these findings do not support GSD of the enzyme by electrostatic frustration.⁵⁵

Enzyme Flexibility and Domain Movements. The ODCase structure undergoes quite large fluctuations. This is evidenced by the large RMSD from a chosen equilibrium configuration reported in Table 1. This flexibility is consistent with the significant domain movements induced by the binding of inhibitors as inferred from the analysis of X-ray structures.⁵⁶

Hur and Bruice,²⁰ in their molecular dynamics study of YEO, found that decarboxylation is accompanied by a rearrangement of loop 203–218. The loop is located near the substrate phosphate tail, and it is closed by the two hydrogen bonds $203(\text{O}) \cdots 218(\text{HN})$ and $205(\text{NH}) \cdots 218(\text{O})$. Our simulation of YEO confirmed the rearrangement of the loop 203–218 when ODCase/Omp is converted to ODCase/Ump[−]. However, instead of observing the formation of the β -hairpin, we observed the formation of a three-residue long α -helix (residues 211–213) in correspondence of the β -turn reported by Hur and Bruice.²⁰ Regardless of the type of structural rearrangement, which can be attributed to the different force field employed in the two simulations, this finding suggests a significant motion during the decarboxylation that could be relevant for the catalytic activity of the enzyme. Hence, we looked for an analogous rearrangement in the other two ODCase strains. However, within the time scale spanned by our simulations, we have not found any significant rearrangement in the MBTO and ECO structures upon decarboxylation. Therefore, if any structural rearrangement accompanies the process, its contribution to the catalytic proficiency it is not likely relevant.

Protonation at C5. Before concluding this section, we would like to add few remarks on the C5-protonation mechanism proposed by Kollman (Figure 2, reaction 2),²¹ which assumes a neutral Asp70 residue. With this choice, Kollman and collaborators²¹ noticed that Lys72 spends most of its time close to the C5 of Omp and, consequently, proposed a protonation at C5 by Lys72 as the first step of the decarboxylation (Figure 2, reaction 2). Indeed, free-energy perturbation calculations predicted a considerably low decarboxylation barrier for the C5-protonated intermediate.²¹ We performed MD simulations

(55) Lundberg, M.; Blomberg, M. R. A.; Diegbahn, P. E. M. *J. Mol. Model.* **2002**, 8, 119.

(56) Harris, P.; Poulsen, J.-C. N.; Jensen, K. F. *J. Mol. Biol.* **2002**, 318, 1019.

Table 3. Statistical Data on Distances (in Å) between the N ζ -Lys72 (*Methane bacterium thermoautotrophicum*, MBTO, ODCase Numbering) and the C5 Atom of the Omp Substrate for Both Neutral and Charged Asp70^a

		minimum	maximum	average	% less than 4.3 Å
MTBO	Asp-H	3.50	5.32	4.30 (0.46)	58
	Asp [−]	4.24	5.36	4.91 (0.38)	4

^a Standard deviation from the mean is reported in parentheses. In the last column, the probability of having a distance shorter than the average distance calculated in MBTO with a protonated aspartyl group is also shown.

on different protonation states of the active site. Our calculations clearly show that the C5-protonation relies on the assumption of a neutral Asp70, which allows Lys72 to go close to C5 in an optimal position for a hypothetical proton transfer. As Asp70 is deprotonated, this is no longer possible. This can be clearly inferred from Table 3, where some statistical data on distances between N ζ of Lys72 and C5 of the substrate are reported for neutral and ionized Asp70. We remark that Kollman proposed a protonated Asp70 on pK_a obtained via free-energy perturbation calculations.²¹ On the other hand, Warshel, with the same type of calculations but a different computational protocol, predicted a deprotonated Asp70¹⁹ (see also ref 41). Furthermore, as Hur and Bruce have already discussed, the C5 position is surrounded by hydrophobic residues, which protect the carbon from acidic groups.²⁰

In summary, on the basis of the above discussion and the latest experimental evidences, which support a fully ionized conserved array, we rule out a C5 mechanism.

B. QM/MM Simulations of the Decarboxylation Process. Protonation at C6 with Decarboxylation. In an attempt to investigate the possibility of a concerted protonation/decarboxylation, we have chosen as the reaction coordinate the distance between the Lys72 N ζ hydrogen and C6. Indeed, with this choice we have observed a concerted protonation/decarboxylation process (Figure 4). The associated free-energy profile, reported in Figure 4d, is characterized by an activation energy of 138 kJ mol^{−1}, which is considerably higher than the experimental activation energy ($\Delta G^\ddagger = 72$ kJ mol^{−1}).³ A different choice of the N ζ hydrogen does not significantly change the free-energy profile reported. However, the choice of a simple linear reaction coordinate for such a complicated process could be inappropriate and therefore lead to an overestimation of the activation energy or to a wrong outcome. We have tried verifying the reliability of our choice by starting six free trajectories from points near the maximum of the free energy. Four of them ended at the reactants, the others at the products. This finding, although not significant from a statistical point of view, gives us confidence that the maximum in the free energy is reliably near the true TS. The high activation energy can be partially attributed to the strong hydrogen-bonding network around the Omp carboxylate. In fact, the protonation of C6 by Lys72 requires first a strong distortion of the active site, as Asp70 lags behind Lys72, and then the breaking of the network. However, we cannot rule out the overestimation of the energy because of our choice of the reaction coordinate.

Direct Decarboxylation without Prior Protonation. To study the direct decarboxylation without prior protonation, the C6–COO[−] distance, d , was chosen as reaction coordinate. The calculated free energy profile for the process, reported in Figure

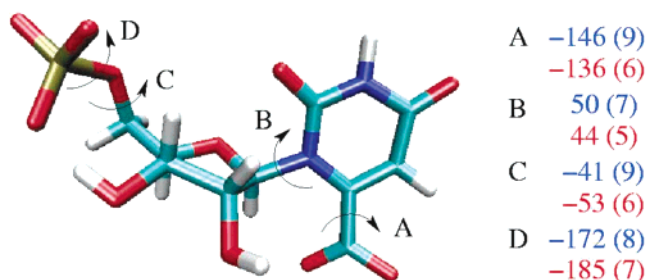


Figure 6. Selected dihedral angles as calculated from QM/MM simulations of Omp in aqueous solution (blue entries) and in the enzyme cavity (red entries). Values obtained from classical molecular dynamics are qualitatively similar.

5, is characterized by a monotonic energy increase as the C–C bond breaks. The activation free energy is, therefore, practically equal to the dissociation energy of the C–C bond. Two distinct steps are present, corresponding to the breaking of the C–C bond ($d = 1.8$ Å, Figure 5b) and the breaking of the H-bonds between the forming CO₂ moiety and the two coordinating lysines ($d = 2.0$ Å, Figure 5c). The CO₂ moiety reaches a linear conformation at about 2.4 Å. Once the CO₂ is released, it drifts away and it is captured from hydrophobic residues in the β -barrel to which Lys42, Asp70, and Lys72 belong. When the Lys72–Omp hydrogen bond is being broken, Lys72 goes spontaneously close to the C6 atom of the newly formed carboanion with the N ζ H atom in a suitable position for a subsequent protonation attack (Figure 5d).

From Figure 5, it is also evident that the enzyme considerably reduces the activation free energy with respect to the aqueous solution. Taking as the activation free energy, ΔG^\ddagger , the value corresponding to the formation of the linear CO₂ molecule, we estimate $\Delta G_{\text{cat}}^\ddagger = 90$ kJ mol^{−1}. The corresponding quantity in aqueous solution, calculated here with the same computational setup, is $\Delta G_{\text{wat}}^\ddagger = 185$ kJ mol^{−1}. This implies a rate enhancement of the spontaneous decarboxylation by the enzyme of $k_{\text{cat}}/k_{\text{wat}} = 3.5 \times 10^{16}$, which is in agreement with the experimentally proposed $k_{\text{cat}}/k_{\text{wat}} = 1.7 \times 10^{17}$.³ This strongly indicates that the actual enzymatic mechanism involves a direct decarboxylation with a stabilization of the intermediate by Lys72.

The agreement of the calculated $k_{\text{cat}}/k_{\text{wat}}$ value with the experimental value is likely fortuitous. In fact, the activation free energies computed for both the catalyzed reaction and the reaction in water are higher than the experimental values, which are $\Delta G_{\text{cat}}^\ddagger = 72$ kJ mol^{−1} and $\Delta G_{\text{wat}}^\ddagger = 164$ kJ mol^{−1},³ respectively (for the reaction in water only an extrapolation from a homologous series of reactions exists⁵⁷). This overestimation is somehow surprising because it is well known that BLYP exchange and correlation functional tends to underestimate reaction barriers (see, for example, refs 58–60), and it could be a consequence of the choice of the C–C distance as reaction coordinate as discussed before. Also, the fast pulling rate we have adopted could play a role in not allowing the system to relax properly, even though a test simulation with a larger pulling velocity ($v = 1.2$ Å ps^{−1}) has not revealed relevant differences from the free-energy profile here reported.

(57) Snider, M. J.; Wolfenden, R. *J. Am. Chem. Soc.* **2000**, *122*, 11507.

(58) Backer, J.; Andzelm, J.; Muir, M.; Taylor, P. R. *Chem. Phys. Lett.* **1995**, *237*, 53.

(59) Parthiban, S.; de Oliveira, G.; Martin, J. M. L. *J. Phys. Chem. B* **2001**, *105*, 895.

(60) Raugei, S.; Cardini, G.; Schettino, V. *J. Chem. Phys.* **2001**, *114*, 4089.

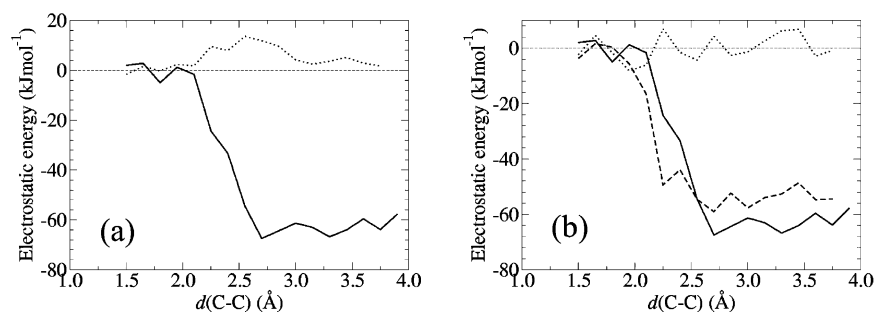


Figure 7. Change in the electrostatic interaction energy as a function of the reaction coordinate. (a) Interaction energy calculated for the Omp/enzyme complex (solid line) and for Omp in aqueous solution (dotted line); (b) interaction energy for the Omp/enzyme complex: total (solid line), between Omp and the residues in the enzyme cavity (dashed line). In (b), the dotted line represents the statistical uncertainty expressed as mean square deviations from the average. The interaction energy has been calculated by charge–charge interactions (see section II.A for details) averaging over five trajectories. The values obtained should be taken only for a qualitative comparison.

In this regard, it must be also pointed out that our calculations neglect the contribution due to the binding of the substrate, which could contribute significantly in the accurate determination of the overall activation free energy (that corresponds to $k_{\text{cat}}/K_{\text{M}}$) as suggested by Miller and Wolfenden.³ It is, however, clear that this possibly missing contribution does not alter the analysis of the results presented here and the conclusions, based on it, remain valid.

C. Ground-State Destabilization versus Transition-State Stabilization. The results reported so far strongly support a direct decarboxylation mechanism with the formation of a carboanionic intermediate. It remains to be assessed whether a GSD or a TSS drives the decarboxylation.

We started noticing that an electrostatic frustration would result in a distortion of the substrate with respect to a relaxed conformation in water. In our classical (Amber) and QM/MM simulations, the Omp geometry in the substrate/enzyme complex resembles very much that of the most stable Omp conformer in water. This can be seen from Figure 6, where selected torsional angles of the substrate are reported. Previous classical (CHARMM) molecular dynamics simulations on YEO by Hur and Bruice²⁰ suggested a similar resemblance of the Omp structures. These considerations, along with the extraordinary stability of the charged network discussed above, play against a GSD mechanism.

To further address the issue, we have calculated the electrostatic interaction energy between Omp and the enzyme as the reaction proceeds (Figure 7). As the enzyme-catalyzed reaction progresses, there is a considerable decrease in the electrostatic energy, which is not present for the uncatalyzed reaction (Figure 7a). The decrease of the electrostatic energy starts after the breaking of the C–C bond, and it is almost concerted with the cleavage of the H-bond between Lys72 and the CO₂ moiety as can be inferred by comparing Figures 5 and 7. In fact, the electrostatic stabilization appears to be essentially due to the charged residues of the conserved array (Figure 7b). We would like to remark that, although the statistical uncertainty on the electrostatic energy as calculated by averaging over all of the steering dynamics trajectories is large (Figure 7b), the observed energy decrease is meaningful.

The calculated trend of the electrostatic interaction energy suggests an extremely important role in the catalysis for Lys72, which is able to stabilize the developing negative charge at C6, and therefore the TS or, equivalently, the intermediate, and eventually provides the proton that saturates the valence of the

C6 atom of Ump⁻. Of course, water cannot stabilize the developing C6 charge (and therefore the intermediate) equally well.

Support of this proposal comes from the high affinity between the enzyme and the negative charge generated at C6 in the TS, which can be inferred from the favorable interaction between the –O⁻ of the inhibitor BMP in the ECO/BMP complex.^{10,22}

IV. Conclusions

In this paper, we reported an extensive examination of the most convincing catalytic mechanisms proposed for ODCase. The lack of structural (experimental) information on the ground state of ODCase/Omp complex is overcome by a careful construction of the model and the analysis of three different strains of the enzyme.

Classical molecular dynamics simulations in the nanosecond time scale along with hybrid Car–Parrinello/Molecular mechanics simulations suggest that the remarkable catalytic proficiency of orotidine monophosphate decarboxylase is caused by an electrostatic stabilization of the TS, strongly supporting the concept of preorganization energy by Warshel.¹⁹ In particular, the fully conserved Lys72 (MTBO numbering) largely contributes to the stabilization of the TS or, equivalently, of the carboanionic intermediate, as also proposed by Hur and Bruice.²⁰

No evidence of GSD was found as (i) the geometry of the substrate in the enzyme cavity resembles very much that of the most stable conformer in aqueous solution, and (ii) the H-bond network accommodating the substrate is remarkably stable. In addition to Lys72 (MTBO numbering),^{9,19,20} also Lys42 turned out to interact with the carboxyl moiety of the substrate, which strongly contributes to shield the Omp carboxylate from the forming Asp70. This feature is common to all of the ODCase/Omp complexes investigated. Furthermore, the proposal by Kollman and co-workers²¹ that decarboxylation is anticipated by protonation at C5 by Lys72 is not substantiated by our findings. If fact, this mechanism strongly relies on a protonated Asp70, which is ruled out by the most recent experimental evidence.

Finally, decarboxylation is accompanied by a significant structural rearrangement in the isoenzyme from YEO, but not in that from MTBO and ECO, suggesting that protein relaxation after decarboxylation is not likely to be crucial for the catalysis.²⁰

Acknowledgment. We are grateful to the MURST Cofin for financial support and to the INFN/CINECA for a large computer grant. We thank Dr. S. Pantano for many useful discussions.

JA0455143